

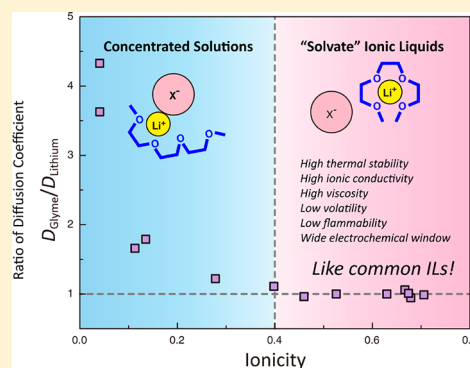
Glyme–Lithium Salt Equimolar Molten Mixtures: Concentrated Solutions or Solvate Ionic Liquids?

Kazuhide Ueno, Kazuki Yoshida, Mizuho Tsuchiya, Naoki Tachikawa, Kaoru Dokko, and Masayoshi Watanabe*

Department of Chemistry and Biotechnology, Yokohama National University, 79-5 Tokiwadai, Hodogaya-ku, Yokohama 240-8501, Japan

S Supporting Information

ABSTRACT: To demonstrate a new family of ionic liquids (ILs), i.e., “solvate” ionic liquids, the properties (thermal, transport, and electrochemical properties, Lewis basicity, and ionicity) of equimolar molten mixtures of glymes (triglyme (G3) and tetraglyme (G4)) and nine different lithium salts (LiX) were investigated. By exploring the anion-dependent properties and comparing them with the reported data on common aprotic ILs, two different classes of liquid regimes, i.e., ordinary concentrated solutions and “solvate” ILs, were found in the glyme–Li salt equimolar mixtures ($[\text{Li}(\text{glyme})]\text{X}$) depending on the anionic structures. The class a given $[\text{Li}(\text{glyme})]\text{X}$ belonged to was governed by competitive interactions between the glymes and Li cations and between the counteranions (X) and Li cations. $[\text{Li}(\text{glyme})]\text{X}$ with weakly Lewis basic anions can form long-lived $[\text{Li}(\text{glyme})]^+$ complex cations. Thus, they behaved as typical ionic liquids. The lithium “solvate” ILs based on $[\text{Li}(\text{glyme})]\text{X}$ have many desirable properties for lithium-conducting electrolytes, including high ionicity, a high lithium transference number, high Li cation concentration, and high oxidative stability, in addition to the common properties of ionic liquids. The concept of “solvate” ionic liquids can be utilized in an unlimited number of combinations of other metal salts and ligands, and will thus open a new field of research on ionic liquids.



1. INTRODUCTION

Owing to their interesting physicochemical properties, ionic liquids (ILs) have received considerable attention in recent years, both as alternatives to conventional organic solvents^{1–3} and as novel electrolytes for future power sources and electrochemical devices.^{4,5} One of the most intensively studied topics in this burgeoning field is the use of ILs for lithium secondary batteries. ILs are typically used as nonflammable solvents for the sake of battery safety. Because typical aprotic ILs consisting of organic cations such as tetraalkylammonium/phosphonium and fluorinated anions are electrochemically inert in lithium batteries, numerous aprotic IL–Li salt binary mixtures have been tested with a variety of anode and cathode materials.^{6–10} However, the use of aprotic IL-based electrolytes has not yet been established in practical lithium secondary batteries because of certain major issues, including a high viscosity, low Li^+ concentration, low Li^+ transference number, and concentration polarization during charge–discharge.¹¹ These disadvantages arise mainly from the fact that the two cations (i.e., the IL and Li cations) are present in the same electrolyte.

To address the issues mentioned above, lithium ionic liquids that only possess a lithium cation as the cationic species have been designed.^{12,13} Whereas lithium salts possibly become high-melting salts because of strong Coulombic interactions between the Li cation and counteranions, it was possible to prepare

room-temperature fused lithium salts by employing bulky borate anions with two electron-withdrawing groups and two oligoether groups. The former groups attenuate the electron density of the borate center and the latter groups coordinate Li cations. By using a similar strategy, alkali metal oligoether carboxylates have also been reported.¹⁴ However, these fused salts of alkali metals were highly viscous and poorly dissociative, leading to a very low ionic conductivity. In these salts, the coordinating oligoethers were immobilized on the anion, so that the Li cation was trapped in proximity to the anion center. This caused intermolecular ionic association. The bulkiness of the counteranions and the strong Coulombic interaction between the ions may be responsible for their very high viscosity.

Mixtures of oligoethers (with the chemical formula of $\text{CH}_3(\text{CH}_2\text{CH}_2\text{O})_n\text{CH}_3$, the so-called glymes) with Li salts have been widely studied as a model of poly(ethylene oxide) (PEO)-based polymer electrolytes.^{15–18} It was found that some of their stoichiometric mixtures formed structurally well-defined complexes with relatively low melting temperatures below 100 °C.^{19–23} Recently, Angell et al. categorized ionic liquids into four groups: aprotic, protic, inorganic, and solvate (or chelate) ionic liquids.²⁴ Out of these IL families, the

Received: July 26, 2012

Published: August 16, 2012



“solvate” ionic liquids, where ligand molecules as a third component strongly coordinate the cation and/or anion of salts, thereby forming complex ions, would be a new family and an important class of ionic liquids, especially for preparing ILs based on metal cations. In light of this classification, the low-melting glyme–Li salt complexes must be a representative of “solvate” ionic liquids. The concept of the $[\text{Li}(\text{glyme})]^+$ complex cation is similar to that for common anions of ILs such as BF_4^- , AlCl_4^- , and PF_6^- ; these ions are the adducts of a Lewis acid (Li^+ for the $[\text{Li}(\text{glyme})]$ cation and BF_3 , AlCl_3 , and PF_5 for the common anions) and Lewis base (glyme for the $[\text{Li}(\text{glyme})]$ cation and F^- and Cl^- for the common anions).

Smyrl et al. first pointed out that glyme–Li salt equimolar mixtures composed of tetraglyme (G4), lithium bis-(trifluoromethanesulfonyl)amide ($[\text{Li}(\text{TFSA})]$), and lithium bis-(pentafluoroethanesulfonyl)amide ($[\text{Li}(\text{BETI})]$) yield ionic liquids,²⁵ which are abbreviated in a way similar to typical ILs ($[\text{Li}(\text{G4})][\text{TFSA}]$, for instance). We previously found that the equimolar mixtures of triglyme (G3) or G4 with lithium fluorosulfonylamide salts such as $[\text{Li}(\text{TFSA})]$,^{26,27} lithium bis-(fluorosulfonyl)amide ($[\text{Li}(\text{FSA})]$),²⁸ and a Li salt of a cyclic TFSA derivative ($[\text{Li}(\text{CTFSA})]$),²⁹ differ from the diluted solutions containing the excess glymes, but show IL-like behaviors such as high thermal stability, low volatility, and low flammability. The preferable electrochemical and Li^+ transport properties for lithium battery electrolytes have also been achieved; the electrochemical oxidative stability was improved as high as approximately 5 V versus Li/Li^+ as compared to approximately 4 V versus Li/Li^+ for the dilute solutions.³⁰ The limiting current density as a result of the Li^+ transport was an order of magnitude higher than that for a typical aprotic IL–Li salt binary mixture.³¹ Consequently, these equimolar mixtures were proved to be effective electrolytes in lithium secondary batteries using LiCoO_2 ,^{30,32} LiFePO_4 ,^{28,32} and elemental sulfur³³ as the cathode, and graphite^{28,32} and $\text{Li}_4\text{Ti}_5\text{O}_{12}$ ³² as the anode.

As in the case of aprotic ILs,³⁴ the properties of glyme–Li salt mixtures may be significantly affected by their anionic structures. Henderson et al. already reported the phase diagrams³⁵ and crystal structures^{20–22} of glyme–Li salt mixtures with different anions. However, the anion dependency on the ion transport and electrochemical properties, which are important in terms of using a molten glyme–Li salt equimolar mixture as a battery electrolyte, has not yet been studied in detail. The transport properties for “solid-state” glyme– LiAsF_6 complexes have also been investigated by Bruce’s group.³⁶ In this paper, the physicochemical properties for equimolar mixtures of glymes and Li salts, $[\text{Li}(\text{G3})]\text{X}$ and $[\text{Li}(\text{G4})]\text{X}$, including nitrate (NO_3^-), trifluoromethanesulfonate ($[\text{OTf}]^-$), tetrafluoroborate (BF_4^-), perchlorate (ClO_4^-), trifluoroacetate ($[\text{TFA}]^-$), $[\text{BETI}]^-$, and $[\text{FSA}]^-$ as X, were studied in a liquid (or supercooled liquid) state and compared with those for the previously reported equimolar mixtures such as $[\text{Li}(\text{glyme})][\text{TFSA}]$ ²⁷ and $[\text{Li}(\text{G3})][\text{FSA}]$.²⁸ The dependence of the ionic structure on the properties was evaluated in terms of the “ionicity” concept for ILs.³⁷ We also performed a comparative analysis of the properties for $[\text{Li}(\text{glyme})]\text{X}$ and the conventional aprotic ILs³⁸ in order to verify their differences and similarities. Finally, we discuss the question in the title of this paper: whether these glyme–Li salt equimolar molten mixtures can indeed be regarded as “solvate” ionic liquids or are simple concentrated solutions of the Li salts in the glyme solvents.

2. EXPERIMENTAL SECTION

Materials. Purified glymes, triglyme (G3) and tetraglyme (G4), and battery-grade Li salts, $[\text{Li}(\text{BETI})]$, $[\text{Li}(\text{OTf})]$, LiBF_4 , and LiClO_4 , were purchased from Kishida Chemical, and $[\text{Li}(\text{FSA})]$ was obtained from Dai-ichi Kogyo Seiyaku. The other Li salts, LiNO_3 and $[\text{Li}(\text{TFA})]$ from Aldrich, were dried under high vacuum at an elevated temperature prior to use. Glyme–lithium equimolar mixtures were prepared by mixing stoichiometric lithium salt and glyme in an Ar-filled glovebox (H_2O , $[\text{H}_2\text{O}] < 1 \text{ ppm}$). Typically, the lithium salt and glyme were mixed and magnetically stirred in a vial at 60 °C overnight. When necessary, the samples were further heated to 80 °C for several hours to ensure a complete mixing of the Li salt and glyme.

Measurements. The melting point (T_m) and glass transition temperature (T_g) were determined using a differential scanning calorimeter (DSC6220, Seiko). The samples were hermetically sealed in aluminum pans in the glovebox. The sample pans were first heated at 70 °C for 10 min, followed by cooling to -150 °C, and then heated from -150 to 70 °C at a scan rate of 10 °C min^{-1} under a nitrogen atmosphere. T_m and T_g were determined from the onset temperatures of the heating thermograms. A thermogravimetric analysis was performed on a TG/TDA 6200 (Seiko) from room temperature to 550 °C at a heating rate of 10 °C min^{-1} under a nitrogen atmosphere. In this study, the thermal decomposition temperature (T_d) was defined as the temperature of a 5% mass loss in the thermogravimetric curves. The ionic conductivity was measured using the complex impedance method in the frequency range of 500 kHz–1 Hz with 10 mV amplitude (VMP2, Princeton Applied Research). Two platinum black electrodes (CG-511B, TOA Electronics, cell constant = approximately 1 cm^{-1}) were dipped in the mixture, and the sample cell was thermally equilibrated at each temperature for at least 90 min using a thermostat chamber. The temperature dependences of the viscosity and density were measured using SVM3000 (Anton Paar). Pulsed-gradient spin-echo nuclear magnetic resonance (PGSE-NMR) measurements were performed using a JEOL AL400 spectrometer with a 9.4 T narrow bore superconducting magnet equipped with a JEOL pulse field gradient probe and current amplifier to study the self-diffusion coefficients of each component in the glyme–lithium salt mixtures: glymes (^1H , 399.7 MHz), fluorinated anions (^{19}F , 376.1 MHz), and lithium cations (^7Li , 155.3 MHz). The experimental procedure for PGSE-NMR has been described in detail in a separate study.²⁷ The Lewis basicity was evaluated from the maximum ultraviolet–visible (UV–vis) absorption wavelength (λ_{Cu}) of a copper complex solvatochromic indicator, (acetylacetonate)(N,N,N',N' -tetramethylethylenediamine) copper(II) tetraphenylborate, $[\text{Cu}(\text{acac})(\text{tmen})][\text{BPh}_4]$,³⁹ dissolved in $[\text{Li}(\text{glyme})]\text{X}$. The oxidative electrochemical stability was studied using linear sweep voltammetry (LSV) at a scan rate of 1 mV s^{-1} in a three-electrode cell, with Li metal foils as the counter and reference electrodes, and a platinum disk (1 mm in diameter) encapsulated in a fluorinated shrinkable tube as the working electrode.

3. RESULTS AND DISCUSSION

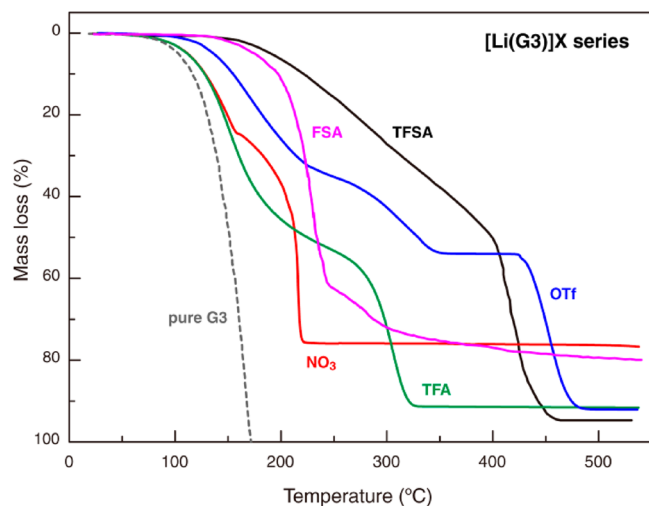
Thermal Stabilities. Table 1 summarizes the thermal properties (T_g , T_m , and T_d) of $[\text{Li}(\text{G3})]\text{X}$ and $[\text{Li}(\text{G4})]\text{X}$ with different anions. $[\text{Li}(\text{G3})][\text{BETI}]$ ($T_m = 74$ °C),²² $[\text{Li}(\text{G3})]\text{BF}_4$ ($T_m = 90$ °C),²⁰ and $[\text{Li}(\text{G3})]\text{ClO}_4$ ($T_m = 103$ °C)²⁰ are

Table 1. Thermal Properties of [Li(G3)]X and [Li(G4)]X^a

glyme–Li salt mixture	T_g (°C)	T_m (°C)	T_d (°C)
[Li(G3)][TFSA]	n.d.	23	190
[Li(G3)][FSA]	n.d.	56	174
[Li(G3)][OTf]	n.d.	35	136
[Li(G3)]NO ₃	−69	27	112
[Li(G3)][TFA]	−85	n.d.	112
[Li(G4)][TFSA]	−54	n.d.	204
[Li(G4)][CTFSA]	n.d.	28	247
[Li(G4)][FSA]	n.d.	23	194
[Li(G4)][BETI]	n.d.	23	227
[Li(G4)]ClO ₄	−51	28	181
[Li(G4)]BF ₄	−63	39	161
[Li(G4)]NO ₃	−70	n.d.	147
[Li(G4)][TFA]	−85	n.d.	149

^aData for [Li(G3)][TFSA] and [Li(G4)][TFSA] are from ref 27. Data for [Li(G3)][FSA] and [Li(G4)][CTFSA] are from refs 28 and 26, respectively.

solid at room temperature. For [Li(G4)][OTf], no homogeneous liquid could be obtained because phase separation occurred at room temperature. Therefore, these samples were excluded from further measurements. In each sample, T_g and T_m are different from those for the pure glymes (also see Supporting Information, Figure S1). Most of the glyme–Li salt mixtures did not readily crystallize, and they remained in a liquid state for several weeks, even though the T_m values of the samples were slightly higher than room temperature. The physicochemical properties could thus be studied in the supercooled states. The thermogravimetric (TG) curves exhibit multistep decreases in weight, as seen in Figure 1 and Figure S2

**Figure 1.** TG curves for [Li(G3)]X.

(Supporting Information). The T_d values of the mixtures are higher than those for pure G3 ($T_d = 103$ °C) and G4 ($T_d = 133$ °C). The first weight loss corresponds to the volatilization of the glymes because the onset temperature is lower than the decomposition temperature of each Li salt. The following steps probably include further evaporation of the glymes through the formation of more-concentrated stoichiometry in certain cases (e.g., [Li(G3)_{1/2}][OTf] and [Li(G3)_{2/3}][OTf]),²⁰ and the decomposition of the lithium salts. As seen in Table 1, T_g and T_d strongly depend on the anions, which suggests that the

glyme–Li cation interaction varies with the anionic structure. Further discussion of the relation of the thermal properties with the anion-dependent ionicity will be given in a later section.

Transport Properties. The transport properties (viscosity η , density ρ , molar concentration c , and ionic conductivity σ) of [Li(G3)]X and [Li(G4)]X at 30 °C are listed in Table 2. The

Table 2. Viscosity (η), Density (ρ), Molar Concentration (c), and Ionic Conductivity (σ) at 30 °C, and Maximum Absorption Wavelength (λ_{Cu}) of the Solvatochromic Indicator, [Cu(acac)(tmen)][BPh₄], for [Li(G3)]X and [Li(G4)]X^a

glyme–Li salt mixture	η (mPa s)	ρ (g cm ^{−3})	c (mol dm ^{−3})	σ (mS cm ^{−1})	λ_{Cu} (nm)
[Li(G3)][TFSA]	169	1.42	3.06	1.1	544
[Li(G3)][FSA]	139	1.36	3.71	1.7	549
[Li(G3)][OTf]	381	1.30	3.90	0.30	562
[Li(G3)]NO ₃	206	1.18	4.77	0.31	558
[Li(G3)][TFA]	83	1.20	4.04	0.096	608
[Li(G4)][TFSA]	81	1.40	2.75	1.6	544
[Li(G4)][CTFSA]	132	1.40	2.98	0.80	540
[Li(G4)][FSA]	111	1.32	3.23	1.4	547
[Li(G4)][BETI]	130	1.46	2.39	0.91	536
[Li(G4)]ClO ₄	644	1.27	3.85	0.40	535
[Li(G4)]BF ₄	314	1.22	3.87	0.50	534
[Li(G4)]NO ₃	172	1.17	4.03	0.26	559
[Li(G4)][TFA]	80	1.19	3.48	0.083	605

^aThe data, except for the λ_{Cu} values of [Li(G3)][TFSA] and [Li(G4)][TFSA], are from ref 27. The data for [Li(G3)][FSA] and [Li(G4)][CTFSA] are from refs 28 and 26, respectively.

temperature dependencies of these properties are also shown in Supporting Information (Figures S3, S4, and S5 for ρ , η , and σ , respectively). [Li(G4)]X have lower values of η , ρ , and c as compared to those for [Li(G3)]X with the same anion. The viscosities range from 80 to 644 mPa s, which are lower than those for the reported lithium ILs^{12,13} and similar to those for aprotic ILs.³⁸ The mixtures with the TFA anion are the least viscous for [Li(glyme)]X, and the mixtures with [TFSA][−] and its derivative anions become less viscous as compared with the other mixtures. The low molecular weight and nonhalogenated NO₃[−] mixtures have lower density values, leading to higher salt (lithium) concentrations, c (up to 4.77 mol dm^{−3} for [Li(G3)]NO₃). Despite the lowest viscosity and high salt concentration, [Li(glyme)][TFA] shows a very low ionic conductivity of less than 0.1 mS cm^{−1}. In contrast, the conductivities of less viscous [Li(glyme)]X with [TFSA][−] and [FSA][−] anions exceed 1 mS cm^{−1}. This difference in the conductivities between [Li(glyme)]X with [TFA][−], and the [TFSA][−] and [FSA][−] anions is ascribed to the magnitude of the dissociativity (or ionicity) of these mixtures (vide infra).

It is known that the maximum absorption wavelength (λ_{Cu}) of a solvatochromic probe, [Cu(acac)(tmen)][BPh₄], shown in the rightmost column of Table 2, gives a good correlation with Gutmann's donor number (DN) for a molecular solvent, where a higher λ_{Cu} indicates a stronger donor property.³⁹ In the case of a typical aprotic IL, λ_{Cu} is predominantly governed by the anionic structure and is almost independent of the cationic structure.³⁸ This is likely the case in [Li(glyme)]X, if [Li(glyme)]⁺ is a stable complex cation. [Li(G3)]X and [Li(G4)]X with the same anion have almost the same λ_{Cu} values. Thus, this polarity scale appears to be indicative of the

Lewis basicity of the anions in the glyme–Li salt equimolar mixtures. The order of the λ_{Cu} values depended on the anions: $\text{ClO}_4^- \sim \text{BF}_4^- < [\text{BETI}]^- < [\text{CTFSA}]^- < [\text{TFSA}]^- < [\text{FSA}]^- < [\text{OTf}]^- < \text{NO}_3^- < [\text{TFA}]^-$. In the aprotic ILs, there was a good correlation between λ_{Cu} and ionicity.³⁸ A higher λ_{Cu} value for the anions is indicative of more enhanced interionic attraction with the cations, leading to lower ionicity. We attempt to confirm this relationship in the glyme–Li salt equimolar mixtures in a later section.

Ionicity and Lithium Transference Number. The molar conductivity ratio ($\Lambda_{\text{imp}}/\Lambda_{\text{NMR}}$) has been used to estimate the degree of dissociation of lithium salts in organic solvents,⁴⁰ and it would be a useful metric for quantifying the ionicity (i.e., how ionic are ILs? or the apparent dissociativity) even in extremely concentrated systems like ILs.³⁸ Here, Λ_{imp} is the molar conductivity measured by the ac impedance method, and Λ_{NMR} can be calculated from the ionic self-diffusion coefficients of cations (D_+) and anions (D_-) measured by PGSE-NMR using the Nernst–Einstein equation

$$\Lambda_{\text{NMR}} = \frac{F^2}{RT}(D_+ + D_-)$$

where F is the Faraday constant, R is the gas constant, and T is the absolute temperature. For the present $[\text{Li}(\text{glyme})]\text{X}$ systems, D_+ and D_- denote the diffusion coefficients of lithium (D_{Li}) and the anions (D_{X}), respectively. This equation postulates that all the diffusing species (Li and X in the case of $[\text{Li}(\text{glyme})]\text{X}$) detected by the PGSE-NMR contribute to the molar conductivity. In contrast, Λ_{imp} relies on the net migration of charged species in an electric field. Therefore, the ratio $\Lambda_{\text{imp}}/\Lambda_{\text{NMR}}$ accounts for the proportion of ions (charged species) that participate in ionic conduction from all the diffusing species on the time scale of the measurement and appears to be a good metric to diagnose the interionic interactions or the correlation of ionic motion.^{41,42}

Because the diffusion measurement using PGSE-NMR is restricted to the NMR-active nuclei, the $\Lambda_{\text{imp}}/\Lambda_{\text{NMR}}$ ratio was not available for $[\text{Li}(\text{glyme})]\text{NO}_3$ and $[\text{Li}(\text{G4})]\text{ClO}_4$ using our NMR probe. Instead, the ionicity was also roughly estimated using another method proposed by Angell et al.⁴³ The Walden plots ($\log \Lambda_{\text{imp}}$ versus $\log \eta^{-1}$) of the ILs were compared with a straight reference line with a slope of unity, the “ideal” KCl line, based on a 1 M KCl aqueous solution. For the ionicity based on Walden plots, we compared the $\Lambda_{\text{imp}}/\Lambda_{\text{ideal}}$ ratio to $\Lambda_{\text{imp}}/\Lambda_{\text{NMR}}$ ⁴⁴ while the original ΔW was given by the vertical difference from the ideal line.⁴⁵ Λ_{ideal} is assumed to be the ideal molar conductivity at a given fluidity, η^{-1} , of the ideal line, i.e., the absolute value of Λ_{ideal} ($\text{S cm}^2 \text{ mol}^{-1}$) is equal to that of η^{-1} (P^{-1}). Indeed, the use of the “ideal” KCl line in a Walden plot in terms of disregarding the hydrodynamic radii of different ions⁴⁶ and the questionable validity of using the KCl aqueous solution as the reference is debatable.⁴⁷ However, we still employ this “ideal” KCl line to roughly assess the ionicity of $[\text{Li}(\text{glyme})]\text{X}$ for the purpose of simplicity. This estimation was supported by our empirical observation; a rough consistency was found between $\Lambda_{\text{imp}}/\Lambda_{\text{NMR}}$ and $\Lambda_{\text{imp}}/\Lambda_{\text{ideal}}$ for the reported aprotic ILs,³⁸ protic ILs,⁴⁴ and glyme–Li salt equimolar mixtures,^{26,29} as shown in Figure S6 (Supporting Information) and Table 3. In this paper, $\Lambda_{\text{imp}}/\Lambda_{\text{ideal}}$ is also used as the ionicity scale, especially for $[\text{Li}(\text{glyme})]\text{NO}_3$ and $[\text{Li}(\text{G4})]\text{ClO}_4$, for which the $\Lambda_{\text{imp}}/\Lambda_{\text{NMR}}$ values are unknown.

Figure 2 shows the Walden plots of $[\text{Li}(\text{G3})]\text{X}$ and $[\text{Li}(\text{G4})]\text{X}$ with different anions. The glyme–Li salt equimolar

Table 3. Self-Diffusion Coefficients of Glymes (D_{G}), Lithium (D_{Li}), and Fluorinated Anions (D_{X}), and Ionicities ($\Lambda_{\text{imp}}/\Lambda_{\text{NMR}}$ and $\Lambda_{\text{imp}}/\Lambda_{\text{ideal}}$) for $[\text{Li}(\text{G3})]\text{X}$ and $[\text{Li}(\text{G4})]\text{X}$ at 30 °C^a

glyme–Li salt mixture	diffusion coefficient ($10^{-7} \text{ cm}^2 \text{ s}^{-1}$)			$\Lambda_{\text{imp}}/\Lambda_{\text{NMR}}$	$\Lambda_{\text{imp}}/\Lambda_{\text{ideal}}$	t_{Li}
	D_{G}	D_{Li}	D_{X}			
$[\text{Li}(\text{G3})][\text{TFSA}]$	0.84	0.89	0.57	0.68	0.62	0.61
$[\text{Li}(\text{G3})][\text{FSA}]$	0.81	0.82	0.89	0.71	0.62	0.48
$[\text{Li}(\text{G3})][\text{OTf}]$	0.52	0.42	0.33	0.28	0.29	0.56
$[\text{Li}(\text{G3})]\text{NO}_3$	1.09	0.61	—	—	0.14	—
$[\text{Li}(\text{G3})][\text{TFA}]$	3.74	0.87	0.73	0.04	0.02	0.54
$[\text{Li}(\text{G4})][\text{TFSA}]$	1.29	1.31	1.22	0.63	0.48	0.52
$[\text{Li}(\text{G4})][\text{CTFSA}]$	0.75	0.78	0.75	0.46	0.35	0.51
$[\text{Li}(\text{G4})][\text{FSA}]$	0.97	0.96	1.22	0.53	0.47	0.44
$[\text{Li}(\text{G4})][\text{BETI}]$	0.82	0.82	0.70	0.67	0.49	0.54
$[\text{Li}(\text{G4})]\text{ClO}_4$	0.24	0.23	—	—	0.67	—
$[\text{Li}(\text{G4})]\text{BF}_4$	0.49	0.44	0.43	0.40	0.40	0.51
$[\text{Li}(\text{G4})]\text{NO}_3$	1.08	0.65	—	—	0.11	—
$[\text{Li}(\text{G4})][\text{TFA}]$	3.12	0.86	0.73	0.04	0.02	0.54

^aThe data for $[\text{Li}(\text{G3})][\text{TFSA}]$ and $[\text{Li}(\text{G4})][\text{TFSA}]$ are from ref 27. The data for $[\text{Li}(\text{G4})][\text{CTFSA}]$ are from ref 26.

mixtures show a wide range of behaviors in terms of the ionicity concept, from “good” ILs to “poor” ILs.⁴³ More quantitatively, the ionicity scale fell into a range of 0.71–0.04 for $\Lambda_{\text{imp}}/\Lambda_{\text{NMR}}$ (from 0.67 to 0.02 for $\Lambda_{\text{imp}}/\Lambda_{\text{ideal}}$). It is obvious that the ionicity scales are less than unity for all the mixtures, suggesting the ionic association or correlated ionic motion, and they largely depend on the anionic structure. From the results of the phase diagram, crystal structure, and Raman spectra of the glyme–Li salt mixtures, Henderson and co-workers described an approximate order for the ionic association strengths of simple LiX salts in glymes: $[\text{BPh}_4]^- < [\text{BETI}]^- \sim [\text{TFSA}]^- \sim \text{SbF}_6^- \sim \text{AsF}_6^- < \text{PF}_6^- < \text{ClO}_4^- \sim \text{I}^- < \text{SCN}^- < \text{BF}_4^- < [\text{OTf}]^- < \text{Br}^- < \text{NO}_3^- < [\text{TFA}]^-$ (left to right more associative).³⁵ Good agreement can be seen between Henderson’s association order and the reverse order of our ionicity scales derived from the physicochemical properties (σ , η , and D) for the glyme–Li salt equimolar mixtures. The order of the ionicity is $[\text{TFSA}]^- \sim [\text{FSA}]^- \sim [\text{BETI}]^- \sim \text{ClO}_4^- > [\text{CTFSA}]^- > \text{BF}_4^- > [\text{OTf}]^- > \text{NO}_3^- > [\text{TFA}]^-$.

On the basis of the association state, the glyme–LiX salt mixtures were classified into ion aggregates (AGG), contact ion pairs (CIP), and solvent-separated ion pairs (SSIP).³⁵ These states can be represented by $[\text{Li}^+(\text{nX}^-)]$ or $[(\text{xEO})\text{Li}^+(\text{mX}^-)]$ for AGG, $[(\text{yEO})\text{Li}^+\text{X}^-]$ for CIP, and $[(\text{zEO})\text{Li}^+][\text{X}^-]$ for SSIP, where $m < n$, $x < y < z$, and EO is the oxyethylene group. For the present $[\text{Li}(\text{G3 or G4})]\text{X}$ equimolar mixtures, it is pointed out that CIP is favorable for $[\text{Li}(\text{G3})]\text{X}$, while $[\text{Li}(\text{G4})]\text{X}$ preferentially forms SSIP.³⁵ More quantitative estimations using the Raman spectra of the $[\text{TFSA}]^-$ anions in $[\text{Li}(\text{G3})][\text{TFSA}]$ and $[\text{Li}(\text{G4})][\text{TFSA}]$ also revealed that the SSIP/CIP ratios were approximately 50/50 and approximately 75/25, respectively.¹⁹ Accordingly, one could expect $[\text{Li}(\text{G3})]\text{X}$ to be more associative than $[\text{Li}(\text{G4})]\text{X}$. However, this does not agree with our results on the ionicity scales: $[\text{Li}(\text{G3})]\text{X}$ appears to have higher ionicities than $[\text{Li}(\text{G4})]\text{X}$ with the same anion (Table 3). The association state (SSIP or CIP) was characterized either in static crystalline states using X-ray crystallography or in solutions by Raman spectroscopy as

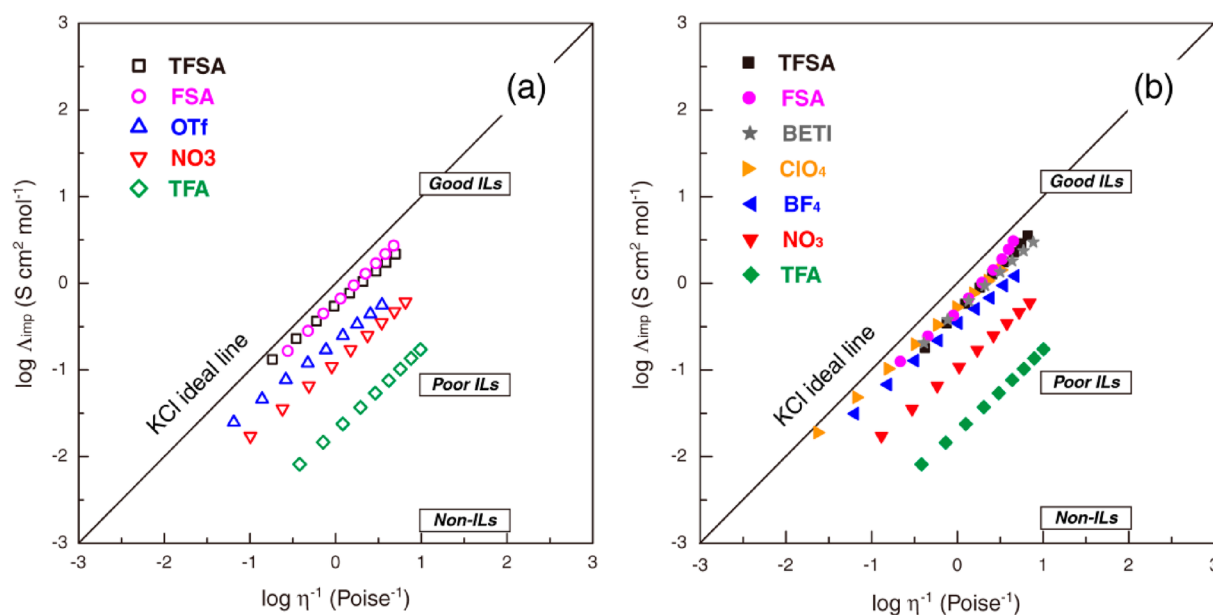


Figure 2. Walden plots for (a) [Li(G3)]X and (b) [Li(G4)]X.

snapshots of the picosecond time scale. Meanwhile, the measurements for the ionicities do not distinguish different association states, but simply detect an average (or equilibrated) state for a longer time scale of amorphous liquids. In contrast to the association states (SSIP and CIP) found in a dilute solution, both the ion pairs should interact closely with their neighbors in highly concentrated systems. Thus, the ionicity scales might be of little relevance to whether SSIP or CIP dominates. The dielectric constants ($\epsilon(\text{G3}) = 7.53$, $\epsilon(\text{G4}) = 7.71$) and donor numbers ($\text{DN}(\text{G3}) = 14.0$, $\text{DN}(\text{G4}) = 16.6$)¹⁵ are unlikely to account for the difference in ionicity between [Li(G3)]X and [Li(G4)]X. The higher ionicity for [Li(G3)]X could possibly be explained by the shorter Li–O distance (i.e., stronger Li⁺–EO interaction) of the [Li(G3)] cation (1.968–2.009 Å) compared to that of the [Li(G4)] cation (2.114–2.189 Å), obtained by *ab initio* MO calculation.^{30,48,49} However, we have not yet reached a definitive conclusion on this discrepancy.

The PGSE-NMR measurements also made it possible to estimate the transference number of lithium (t_{Li}) by

$$t_{\text{Li}} = \frac{D_{\text{Li}}}{D_{\text{Li}} + D_{\text{X}}}$$

It should be noted that the values of t_{Li} found by PGSE-NMR include the transport from both associated and dissociated species. As shown in the rightmost column of Table 3, the t_{Li} value for every [Li(glyme)]X is close to 0.5, some of which may detect the contribution from the diffusion of the neutral ion pair. In such a case, it is not equivalent to the real lithium ion transference number. However, in more dissociated cases such as [Li(glyme)][TFSA], these t_{Li} values are clearly higher than those for the common nonaqueous electrolytes used for lithium batteries⁴⁰ and for an aprotic IL–Li salt binary system with similar viscosity (40–130 mPa s at 30 °C)⁵⁰ measured using the same technique. The high t_{Li} with the high ionicity and high lithium concentration can cover the slower lithium transport caused by high viscosity and would be a favorable aspect for alternative lithium battery electrolytes to replace common nonaqueous systems.³¹

Are the [Li(glyme)]X Mixtures “Solvate” Ionic Liquids?

Here, we first compare the ionicity of [Li(glyme)]X to those of the aprotic ILs with the same anions. We then summarize the correlation between the properties and ionicities for [Li(glyme)]X mixtures in a way similar to that used for aprotic ILs in the previous work.³⁷ This approach may help us to evaluate whether the glyme–Li salt mixtures can be classified as “solvate” ILs.

As noted before, the ionicity scales were influenced by the anionic structures; [Li(glyme)]X with weakly Lewis basic anions has a higher ionicity value (Table 3). More noteworthy is that the ionicities for [Li(glyme)]X with different anions varied over a significantly wide range ($0.04 < \Lambda_{\text{imp}}/\Lambda_{\text{NMR}} < 0.71$, and $0.02 < \Lambda_{\text{imp}}/\Lambda_{\text{ideal}} < 0.67$), as opposed to the case for [C₄mim]-based aprotic ILs, cf. the $\Lambda_{\text{imp}}/\Lambda_{\text{NMR}}$ ($\Lambda_{\text{imp}}/\Lambda_{\text{ideal}}$) values are 0.61 (0.55) for [C₄mim][TFSA], 0.63 (0.57) for [C₄mim][BETI], 0.64 (0.67) for [C₄mim]BF₄, 0.57 (0.55) for [C₄mim][OTf], and 0.52 (0.49) for [C₄mim][TFA].³⁸ The ionicities of [Li(glyme)][TFSA] and [Li(G4)][BETI] are comparable to those for [C₄mim]-based aprotic ILs with the same anion. However, the ionicities for [Li(glyme)][TFA] mixtures suggest that they form mostly neutral species made up of ion pairs or ion aggregates (i.e., “poor” ILs), while the ionicity of [C₄mim][TFA] remains relatively high. In the glyme–Li salt mixtures, the glyme and counteranions compete to interact with the Li⁺ cation. When the donor property (or Lewis basicity) of the anion is very strong, the Li cation prefers to interact with the anions rather than with the glyme. As a result, neutral ion pairs (Li–X), leading to low ionicities, may be formed instead of the intended [Li(glyme)] complex cations. In typical aprotic ILs, there is no such competition, and only the net anion–cation interaction dominates the ionicity. Thus, the balance of the interplays between the three components (glyme–Li⁺–X[−]) is responsible for the remarkable variation in the ionicity in [Li(glyme)]X.

Figure 3 shows the relationship between the λ_{Cu} (Lewis basicity) values of the glyme–Li salt mixtures and the ionicity scales. For the LiNO₃ and LiClO₄ mixtures, where PGSE-NMR was not applicable to the anions, we used $\Lambda_{\text{imp}}/\Lambda_{\text{ideal}}$ for their ionicity scales. Analogous to the case for aprotic ILs,³⁸ the

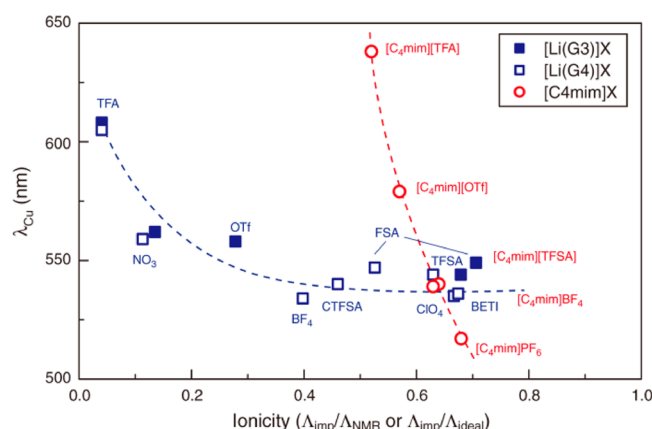


Figure 3. Relationship between ionicity scales and λ_{Cu} values for [Li(glyme)]X and [C₄mim]X. $\Lambda_{\text{imp}}/\Lambda_{\text{ideal}}$ was used for the ionicities of the ClO₄ and NO₃ mixtures. The broken line is a guide for the eye. The data for [C₄mim]X are cited from ref 38.

ionicity increases with decreasing λ_{Cu} from associative [TFA][−], NO₃[−], and [OTf][−] to the more dissociative anions. A high ionicity, comparable to that for typical ILs (>0.4), is obtained for [Li(glyme)]X with λ_{Cu} values lower than 550 nm.

In a detailed comparison with [C₄mim]-based ILs, [Li(glyme)][TFSA], [Li(G4)][BETI], and [Li(G4)]BF₄ (see Table 2) show λ_{Cu} values that are very similar to [C₄mim]-[TFSA] (544 nm), [C₄mim][BETI] (539 nm), and [C₄mim]-BF₄ (540 nm),³⁸ indicating that these anions of [Li(glyme)]X have Lewis basicities that are almost equal to those of the aprotic ILs. In contrast, the λ_{Cu} values in [Li(glyme)]X with stronger Lewis basic anions, [Li(glyme)][TFA] and [Li(G3)][OTf] (Table 2), are lower than those for the [C₄mim]-based ILs with the same anion (λ_{Cu} = 638 and 579 for [C₄mim]-[TFA] and [C₄mim][OTf], respectively).³⁸ In these mixtures, the electron-donating glymes, as well as the anions, may play a role in lowering λ_{Cu} , although we could not determine reliable λ_{Cu} values for the pure G3 and G4, presumably due to the ligand exchange between the ligands of the copper probe and pure glymes. The lower ionicity scales for [Li(glyme)][TFA] and [Li(G3)][OTf] reinforce the idea that the glyme molecules coordinated Li cations only weakly, which in turn affects the λ_{Cu} value of the copper complex probe in these mixtures.

The above discussion suggests that the [Li(glyme)] complex cation may not be formed in certain [Li(glyme)]X mixtures, especially for more associated cases. In the concept of “solvate” ionic liquids, the long-term coordination of Li cations should be assured by the glymes.²⁴ Single-crystal structures of glyme–Li salt complexes would provide strong evidence for this postulation. However, their glass-forming properties appear to make it difficult to perform single-crystal X-ray diffraction measurements. Among the [Li(glyme)]X studied here, single-crystal structures have only been reported for [Li(G3)][OTf]²⁰ and speculated for [Li(G4)]BF₄²¹ and [Li(G4)]ClO₄.²³ Moreover, there is a concern about the attenuation of the Li⁺–EO interaction in the liquid state with elevating temperature. Therefore, we plotted the ratio of the self-diffusion coefficients of the glymes and lithium, $D_{\text{G}}/D_{\text{Li}}$, as a function of the ionicity scales measured in a liquid state to assess the coordination of the Li cations by the glymes.

Figure 4 highlights that the [Li(glyme)]X can be divided broadly into two classes based on the $D_{\text{G}}/D_{\text{Li}}$ ratio. For the dissociated case where the ionicity scale was more than 0.4, the

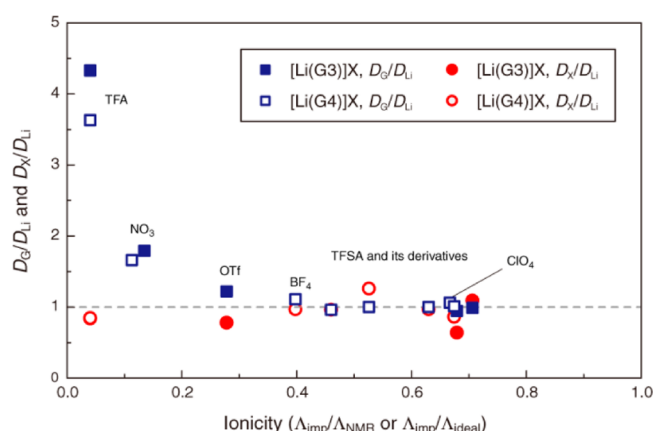


Figure 4. Relationship between ionicity scales and ratio of diffusion coefficients $D_{\text{G}}/D_{\text{Li}}$ and $D_{\text{X}}/D_{\text{Li}}$ for [Li(glyme)]X. $\Lambda_{\text{imp}}/\Lambda_{\text{ideal}}$ was used for the ionicity of the ClO₄ and NO₃ mixtures.

$D_{\text{G}}/D_{\text{Li}}$ ratio is almost unity, suggesting that the Li cation and glyme diffuse together. This result can be seen as a proof of the formation of [Li(glyme)] complex cations in the liquid state. That is to say, these mixtures can be regarded as lithium “solvate” ionic liquids. In more associated mixtures (ionicity <0.4), the glymes (solvents) diffuse faster than the Li cations ($D_{\text{G}}/D_{\text{Li}} > 1$), which resembles the behaviors in common nonaqueous electrolytes.^{40,51} In these associated cases, the Lewis basicity of the anions is higher than or comparable to that of the glymes, and the weaker Li⁺–EO interaction results in a poor complex formation. Hence, they should behave as concentrated solutions. It appears that [Li(G4)]BF₄ ($\Lambda_{\text{imp}}/\Lambda_{\text{NMR}}$ = 0.4) is the dividing line for whether [Li(glyme)]X are “solvate” ILs or concentrated solutions.

As can be seen in Figure 4 and Table 3, the ratio of the self-diffusion coefficients of the anions and lithium, $D_{\text{X}}/D_{\text{Li}}$, is normally less than unity, except for [Li(glyme)][FSA], which indicates a faster diffusion of Li cations compared to the anions. This observation can be separately explained for dissociated and associated mixtures. For the more dissociated [Li(glyme)]X (i.e., lithium “solvate” ILs), it can be understood as the similarity to aprotic ILs, where cations diffuse faster than anions in most cases.³⁴ For [Li(glyme)][FSA], the exceptionally higher $D_{\text{X}}/D_{\text{Li}}$ is presumably attributable to the relatively small size of the FSA anions and the weaker interactions between the cations and FSA anions, as reported for an aprotic FSA-based IL⁵² and its Li salt binary system.⁵³ In contrast, the behaviors in the associated [Li(glyme)]X mixtures appear to be similar to lithium salt solutions in low-polar solvents. Hayamizu et al. reported that faster diffusion of lithium compared to anions has been observed for low-polar organic electrolyte solutions, in which neutral ion pairs of the lithium salts were predominantly formed.⁴⁰

To further validate the two classes, the “solvate” ILs and concentrated solutions, upon changing the anionic structure, we studied the various properties in connection with the ionicity. Figure 5 shows the dependence of the thermal properties on the ionicity. T_{g} is related to the cohesive energy, and T_{d} corresponds to the evaporation of the glymes (Li⁺–EO interactions). These temperatures are available for the whole range of [Li(glyme)]X, and both thermal properties clearly increase with an increase in the ionicity. The lower T_{g} and T_{d} values in the mixtures with lower ionicity arise from the only weakly coordinating glymes. For [Li(glyme)]X with high

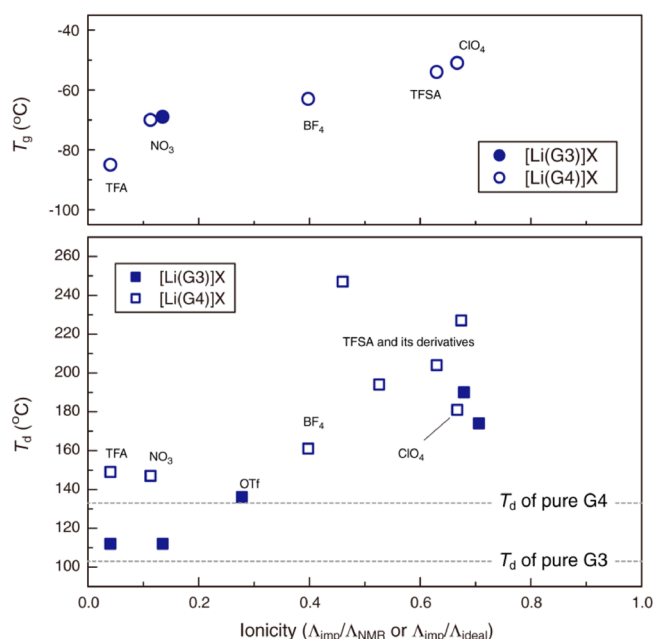


Figure 5. Relationship between ionicity scales and thermal properties, T_g (top) and T_d (bottom), for $[\text{Li}(\text{glyme})]\text{X}$. $\Lambda_{\text{imp}}/\Lambda_{\text{ideal}}$ was used for the ionicity of the ClO_4 and NO_3 mixtures. The broken lines in the bottom figure represent the T_d values of pure G3 and G4.

ionicity, the Coulombic interactions between dissociated $[\text{Li}(\text{glyme})]$ cations and the anions are related to a higher T_g , and the strong Li^+ –EO bindings are reflected in the higher T_d . An intermediate behavior was seen in $[\text{Li}(\text{G3})][\text{OTf}]$ and $[\text{Li}(\text{G4})]\text{BF}_4$, which appears to be in agreement with the findings in Figure 4. Because T_d is dominated by the evaporation of the glymes, an even more dissociated $[\text{Li}(\text{glyme})]\text{X}$ should have lower thermal stability when compared to common aprotic ILs. However, the thermal stability was retained up to approximately 200 °C by the formation of a $[\text{Li}(\text{glyme})]$ complex cation with G4.

Similarly, the viscosity data for $[\text{Li}(\text{glyme})]\text{X}$ are also plotted against the ionicity scales in Figure 6. Because of the strong Coulombic interactions between the dissociated cations and anions, it seems normal for a $[\text{Li}(\text{glyme})]\text{X}$ with a higher ionicity to display a higher viscosity, as indicated by the broken

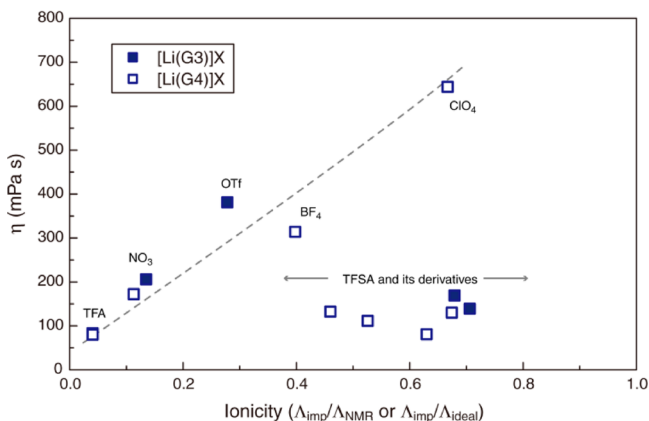


Figure 6. Relationship between viscosity η and ionicity scales for $[\text{Li}(\text{glyme})]\text{X}$. $\Lambda_{\text{imp}}/\Lambda_{\text{ideal}}$ was used for the ClO_4 and NO_3 mixtures. The broken line is a guide for the eye.

line in Figure 6. However, $[\text{Li}(\text{glyme})]\text{X}$ with TFSA and its derivatives (FSA, CTFSA, and BETI) are obviously extraordinary cases; they had low viscosities despite high ionicities. These lower viscosities may be considered to be primarily caused by weaker interactions of TFSA-type anions with cations, as proven by *ab initio* MO calculation for common aprotic ILs.^{53,54}

Finally, we examined the oxidative decomposition potentials for the glyme–Li salt equimolar mixtures because they are greatly associated with their highest occupied molecular orbital (HOMO) energy levels. If stable $[\text{Li}(\text{glyme})]$ complex cations are formed in the mixtures, the strong Li^+ –EO interactions lower the HOMO energy level of the glymes, so that the anodic stability of $[\text{Li}(\text{glyme})]\text{X}$ is improved. Our previous work revealed that $[\text{Li}(\text{G3})][\text{TFSA}]$ has higher oxidative stability than $[\text{Li}(\text{G4})][\text{TFSA}]$ because of the lower HOMO energy of $[\text{Li}(\text{G3})][\text{TFSA}]$ compared to $[\text{Li}(\text{G4})][\text{TFSA}]$, as estimated by an *ab initio* MO calculation.³⁰ Therefore, in more associated $[\text{Li}(\text{glyme})]\text{X}$ mixtures, the glymes that interact with the Li cation only weakly appear to become less stable. Moreover, the oxidative stability of $[\text{Li}(\text{glyme})]\text{X}$ should also depend on the anionic species: strong Lewis basic anions are less stable.^{55–57} Figure 7 shows LSV curves on a Pt electrode for $[\text{Li}(\text{G3})]\text{X}$

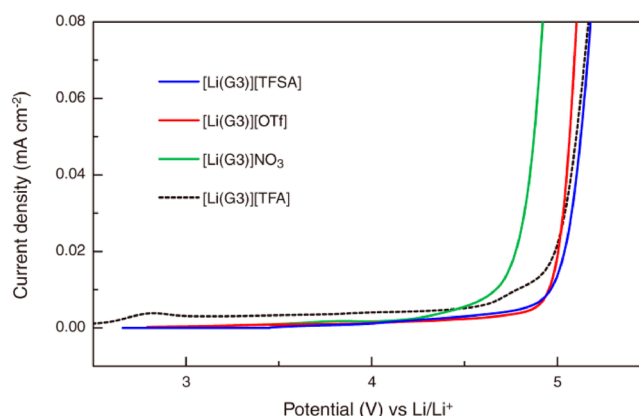


Figure 7. Linear sweep voltammograms of $[\text{Li}(\text{G3})]\text{X}$ at scan rate 1 mV s^{-1} at 30 °C.

mixtures. The modest anodic current in $[\text{Li}(\text{G3})][\text{TFA}]$ indicates that this sample continues to decompose during the potential sweep, although a sharp increase in the anodic current appears at around 5 V versus Li/Li^+ . As expected, the order of the anions for the anodic limit of $[\text{Li}(\text{G3})]\text{X}$ was $[\text{TFSA}]^- > [\text{OTf}]^- > \text{NO}_3^- > [\text{TFA}]^-$. Although we did not distinguish which species among the glymes and the anions were oxidized in the LSV measurements, $[\text{Li}(\text{glyme})]\text{X}$ with strongly Lewis basic anions such as $[\text{TFA}]^-$ and NO_3^- should have lower oxidative stability in either case. The high oxidative stability is favorable for lithium battery electrolytes. $[\text{Li}(\text{glyme})]\text{X}$ with TFSA-type anions are the most suitable among the tested $[\text{Li}(\text{glyme})]\text{X}$, because of their low viscosity, high ionic conductivity, high ionicity, high lithium transference number, and high oxidative stability.

4. CONCLUSIONS

The anionic structure of $[\text{Li}(\text{glyme})]\text{X}$ was varied over a wide range of Lewis basicity values, and its roles in the ionicity and the thermal, transport, and electrochemical properties were studied. Through a systematic study of the property–ionicity

correlations and a comparison to aprotic ILs, we found that [Li(glyme)]X can be divided into two categories, which are dominated by the competitive interactions between the glymes and counteranions and between the glymes and Li cations. In light of the new classification of ILs, we could conclude that [Li(glyme)]X mixtures with weak Lewis basic anions such as TFSA-type anions and ClO₄ behave like ILs, and they are evidently the lithium “solvate” ILs because the formation of [Li(glyme)] complex cations was strongly supported. In [Li(glyme)]X with strong Lewis basic anions, such as [Li(glyme)][TFA] and [Li(glyme)]NO₃, where the anionic interaction with the Li⁺ was stronger than the Li⁺–glyme interaction, the glymes interacted with the Li cations only weakly, and the ionicity became significantly low because of the formation of neutral LiX ion pairs. Therefore, they could be considered as concentrated solutions. Intermediate behaviors were often observed in [Li(G3)][OTf] and [Li(G4)]BF₄. However, [Li(G4)]BF₄ appeared to be closer to the “solvate” ionic liquids based on their λ_{Cu} values and ionicity scales. The BF₄ anion is likely the border dividing the categories.

The facile preparation procedure and low cost of the glyme–Li salt equimolar mixtures would be more advantageous than aprotic IL–Li salt binary systems for a thermally stable lithium-conducting electrolyte. Furthermore, the slow lithium transport as a result of the inherently high viscosity of [Li(glyme)]X may be covered by the high t_{Li} and high lithium concentration. Among the [Li(glyme)]X tested in this work, a combination with bulky TFSA-type anions was preferred in terms of its lower viscosity as well as its high ionicity.

Although we dealt with Li salts and glymes to demonstrate the possibility of developing lithium solvate ionic liquids as lithium-conducting electrolytes, there is obviously potential for forming combinations with other metal salts and ligands, many of which would yield a solvate IL. As solvated anions, the fluorohydrogenate anion [(FH)_{2.3}F]^{−58} and oligomeric acetic acid anion [(AcO)_xH_{x−1}]^{−59} are good examples. This “solvation” strategy is of great interest, because it might realize the preparation of ionic liquids that could not be obtained using the common methods (e.g., ILs composed of multivalent metal ions), and whose properties could be tunable by the proper choice of ligands based on a knowledge of the well-established coordination chemistry. Thus, the concept of “solvate” ILs will open up a new field of research on ionic liquids.

■ ASSOCIATED CONTENT

■ Supporting Information

DSC thermograms, TG curves, the temperature dependences of density, viscosity, and ionic conductivity, and the relationship between $\Lambda_{imp}/\Lambda_{NMR}$ and $\Lambda_{imp}/\Lambda_{ideal}$ for aprotic ILs and [Li(glyme)]X. This material is available free of charge via the Internet at <http://pubs.acs.org>.

■ AUTHOR INFORMATION

Corresponding Author

*Tel./Fax: +81-45-339-3955. E-mail: mwatanab@ynu.ac.jp.

Notes

The authors declare no competing financial interest.

■ ACKNOWLEDGMENTS

This study was supported in part by the Advanced Low Carbon Technology Research and Development Program (ALCA) of the Japan Science and Technology Agency (JST) and by the

Technology Research Grant Program of the New Energy and Industrial Technology Development Organization (NEDO) of Japan.

■ REFERENCES

- (1) Wasserscheid, P.; Keim, W. *Angew. Chem., Int. Ed.* **2000**, *39*, 3772.
- (2) Rogers, R. D.; Seddon, K. R. *Science* **2003**, *302*, 792.
- (3) Plechkova, N. V.; Seddon, K. R. *Chem. Soc. Rev.* **2008**, *37*, 123.
- (4) Galinski, M.; Lewandowski, A.; Stepniak, I. *Electrochim. Acta* **2006**, *51*, S567.
- (5) Armand, M.; Endres, F.; MacFarlane, D. R.; Ohno, H.; Scrosati, B. *Nat. Mater.* **2009**, *8*, 621.
- (6) Garcia, B.; Lavalley, S.; Perron, G.; Michot, C.; Armand, M. *Electrochim. Acta* **2004**, *49*, 4583.
- (7) Sakaebe, H.; Matsumoto, H. *Electrochem. Commun.* **2003**, *5*, 594.
- (8) Chou, S. L.; Wang, J. Z.; Sun, J. Z.; Wexler, D.; Forsyth, M.; Liu, H. K.; MacFarlane, D. R.; Dou, S. X. *Chem. Mater.* **2008**, *20*, 7044.
- (9) Seki, S.; Kobayashi, Y.; Miyashiro, H.; Ohno, Y.; Usami, A.; Mita, Y.; Kihira, N.; Watanabe, M.; Terada, N. *J. Phys. Chem. B* **2006**, *110*, 10228.
- (10) Xu, J. Q.; Yang, J.; NuLi, Y.; Wang, J. L.; Zhang, Z. S. *J. Power Sources* **2006**, *160*, 621.
- (11) Lewandowski, A.; Swiderska-Mocek, A. *J. Power Sources* **2009**, *194*, 601.
- (12) Shobukawa, H.; Tokuda, H.; Tabata, S.; Watanabe, M. *Electrochim. Acta* **2004**, *50*, 305.
- (13) Shobukawa, H.; Tokuda, H.; Susan, M. A. H.; Watanabe, M. *Electrochim. Acta* **2005**, *50*, 3872.
- (14) Zech, O.; Kellermeier, M.; Thomaier, S.; Maurer, E.; Klein, R.; Schreiner, C.; Kunz, W. *Chem.—Eur. J.* **2009**, *15*, 1341.
- (15) Brouillette, D.; Perron, G.; Desnoyers, J. E. *J. Solution Chem.* **1998**, *27*, 151.
- (16) Frech, R.; Huang, W. W. *Macromolecules* **1995**, *28*, 1246.
- (17) Sutjianto, A.; Curtiss, L. A. *J. Phys. Chem. A* **1998**, *102*, 968.
- (18) Rhodes, C. P.; Frech, R. *Macromolecules* **2001**, *34*, 2660.
- (19) Brouillette, D.; Irish, D. E.; Taylor, N. J.; Perron, G.; Odziemkowski, M.; Desnoyers, J. E. *Phys. Chem. Chem. Phys.* **2002**, *4*, 6063.
- (20) Henderson, W. A.; Brooks, N. R.; Brennessel, W. W.; Young, V. G. *Chem. Mater.* **2003**, *15*, 4679.
- (21) Henderson, W. A.; Brooks, N. R.; Young, V. G. *Chem. Mater.* **2003**, *15*, 4685.
- (22) Henderson, W. A.; McKenna, F.; Khan, M. A.; Brooks, N. R.; Young, V. G.; Frech, R. *Chem. Mater.* **2005**, *17*, 2284.
- (23) Grondin, J.; Lassegues, J. C.; Chami, M.; Servant, L.; Talaga, D.; Henderson, W. A. *Phys. Chem. Chem. Phys.* **2004**, *6*, 4260.
- (24) Angell, C. A.; Ansari, Y.; Zhao, Z. F. *Faraday Discuss.* **2011**, *154*, 9.
- (25) Pappenfus, T. M.; Henderson, W. A.; Owens, B. B.; Mann, K. R.; Smyrl, W. H. *J. Electrochem. Soc.* **2004**, *151*, A209.
- (26) Tamura, T.; Yoshida, K.; Hachida, T.; Tsuchiya, M.; Nakamura, M.; Kazue, Y.; Tachikawa, N.; Dokko, K.; Watanabe, M. *Chem. Lett.* **2010**, *39*, 753.
- (27) Yoshida, K.; Tsuchiya, M.; Tachikawa, N.; Dokko, K.; Watanabe, M. *J. Phys. Chem. C* **2011**, *115*, 18384.
- (28) Seki, S.; Takei, K.; Miyashiro, H.; Watanabe, M. *J. Electrochem. Soc.* **2011**, *158*, A769.
- (29) Tamura, T.; Hachida, T.; Yoshida, K.; Tachikawa, N.; Dokko, K.; Watanabe, M. *J. Power Sources* **2010**, *195*, 6095.
- (30) Yoshida, K.; Nakamura, M.; Kazue, Y.; Tachikawa, N.; Tsuzuki, S.; Seki, S.; Dokko, K.; Watanabe, M. *J. Am. Chem. Soc.* **2011**, *133*, 13121.
- (31) Yoshida, K.; Tsuchiya, M.; Tachikawa, N.; Dokko, K.; Watanabe, M. *J. Electrochem. Soc.* **2012**, *159*, A1005.
- (32) Orita, A.; Kamijima, K.; Yoshida, M.; Dokko, K.; Watanabe, M. *J. Power Sources* **2011**, *196*, 3874.
- (33) Tachikawa, N.; Yamauchi, K.; Takashima, E.; Park, J.-W.; Dokko, K.; Watanabe, M. *Chem. Commun.* **2011**, *47*, 8157.

- (34) Tokuda, H.; Hayamizu, K.; Ishii, K.; Abu Bin Hasan Susan, M.; Watanabe, M. *J. Phys. Chem. B* **2004**, *108*, 16593.
- (35) Henderson, W. A. *J. Phys. Chem. B* **2006**, *110*, 13177.
- (36) Zhang, C. H.; Ainsworth, D.; Andreev, Y. G.; Bruce, P. G. *J. Am. Chem. Soc.* **2007**, *129*, 8700.
- (37) Ueno, K.; Tokuda, H.; Watanabe, M. *Phys. Chem. Chem. Phys.* **2010**, *12*, 1649.
- (38) Tokuda, H.; Tsuzuki, S.; Susan, M.; Hayamizu, K.; Watanabe, M. *J. Phys. Chem. B* **2006**, *110*, 19593.
- (39) Muldoon, M. J.; Gordon, C. M.; Dunkin, I. R. *J. Chem. Soc., Perkin Trans. 2* **2001**, 433.
- (40) Hayamizu, K.; Aihara, Y.; Arai, S.; Martinez, C. G. *J. Phys. Chem. B* **1999**, *103*, 519.
- (41) Harris, K. R. *J. Phys. Chem. B* **2010**, *114*, 9572.
- (42) Kashyap, H. K.; Annapureddy, H. V. R.; Raineri, F. O.; Margulis, C. J. *J. Phys. Chem. B* **2011**, *115*, 13212.
- (43) Xu, W.; Cooper, E. I.; Angell, C. A. *J. Phys. Chem. B* **2003**, *107*, 6170.
- (44) Miran, M. S.; Kinoshita, H.; Yasuda, T.; Susan, M. A. B. H.; Watanabe, M. *Phys. Chem. Chem. Phys.* **2012**, *14*, 5178.
- (45) Yoshizawa, M.; Xu, W.; Angell, C. A. *J. Am. Chem. Soc.* **2003**, *125*, 15411.
- (46) MacFarlane, D. R.; Forsyth, M.; Izgorodina, E. I.; Abbott, A. P.; Annat, G.; Fraser, K. *Phys. Chem. Chem. Phys.* **2009**, *11*, 4962.
- (47) Schreiner, C.; Zugmann, S.; Hartl, R.; Gores, H. J. *J. Chem. Eng. Data* **2010**, *55*, 1784.
- (48) Johansson, P.; Gejji, S. P.; Tegenfeldt, J.; Lindgren, J. *Solid State Ionics* **1996**, 86–8, 297.
- (49) Johansson, P.; Tegenfeldt, J.; Lindgren, J. *Polymer* **1999**, *40*, 4399.
- (50) Hayamizu, K.; Aihara, Y.; Nakagawa, H.; Nukuda, T.; Price, W. S. *J. Phys. Chem. B* **2004**, *108*, 19527.
- (51) Hayamizu, K.; Akiba, E.; Bando, T.; Aihara, Y. *J. Chem. Phys.* **2002**, *117*, 5929.
- (52) Fujii, K.; Seki, S.; Fukuda, S.; Kanzaki, R.; Takamuku, T.; Umabayashi, Y.; Ishiguro, S.-i. *J. Phys. Chem. B* **2007**, *111*, 12829.
- (53) Tsuzuki, S.; Hayamizu, K.; Seki, S. *J. Phys. Chem. B* **2010**, *114*, 16329.
- (54) Tsuzuki, S.; Tokuda, H.; Hayamizu, K.; Watanabe, M. *J. Phys. Chem. B* **2005**, *109*, 16474.
- (55) Ue, M.; Murakami, A.; Nakamura, S. *J. Electrochem. Soc.* **2002**, *149*, A1572.
- (56) Johansson, P. *J. Phys. Chem. A* **2006**, *110*, 12077.
- (57) Johansson, P. *Phys. Chem. Chem. Phys.* **2007**, *9*, 1493.
- (58) Hagiwara, R.; Hirashige, T.; Tsuda, T.; Ito, Y. *J. Electrochem. Soc.* **2002**, *149*, D1.
- (59) Johansson, K. M.; Izgorodina, E. I.; Forsyth, M.; MacFarlane, D. R.; Seddon, K. R. *Physical Chemistry Chemical Physics* **2008**, *10*, 2972.